MD3288: Instability latency with controlled noise

S. V. Furuseth, X. Buffat, E. Métral, D. Valuch, B. Salvant, D. Y. Amorim, N. F. Mounet, M. E. Söderén, S. Antipov (CERN, CH-1211 Geneva 23, Switzerland)

T. Pieloni, C. Tambasco (EPFL, CH-1015 Lausanne, Switzerland)

Keywords: external noise, transverse damper, instabilities

Summary

During this MD, performed on June 14th and July 26th, 2018, the latency of single bunch instabilities was tested with an external controllable noise produced by the ADT kicker. The noise acted on a subset of the bunches, whereupon one waited for those bunches to go unstable. The time interval from the moment the noise was turned on to the bunches went unstable was considered the latency of the instability. The latency has been found to be higher for either of the following: weaker noise, higher octupole current, intermediate positive chromaticity, lower transverse damper gain, lower intensity or higher emittance. Based on the bunch and machine parameters, the predicted stability threshold octupole current, in the absence of noise, was calculated with `DELPHI`. The growth from the predicted threshold to the octupole current when the bunches actually went unstable, per minute of active noise, has also been calculated for each bunch. This rate of change of the stability threshold octupole current has been found to be lower for either of the following: weaker noise, higher octupole current or intermediate positive chromaticity. The dependence on the transverse damper gain was inconclusive. The emittance growth rate has been analysed, and indicates that the absolute noise amplitude might have been underestimated by a factor 2.4. The ratio between the noise amplitudes applied on each subset of bunches has been controlled well.

Contents

1 Introduction

The required octupole current to keep the beams in the LHC stable, is typically about a factor 2 larger than what is predicted from the corresponding impedance and beam dynamics model [1]. There have also been multiple observations of long latencies in the development of instabilities in the LHC [2]. That is, bunches become unstable long after the machine parameters were last changed. Latencies of around 40 min have been measured. The delay suggests that the instability was caused by a slow change of the beam distribution. A similar mechanism may have been the cause of longitudinal instabilities observed in the Tevatron at Fermilab [3]. One hypothesis is that such a distribution change is also the cause of the discrepancy between the empirical and theoretical stability threshold of the octupole current.

This experiment was dedicated to measure how the stability threshold would change, in terms of required Landau octupole current, when the beam was continuously affected by an external, coherent, white noise source, driving the modification of the beam distribution. The controlled noise used in the experiment was created by the LHC transverse damper system (ADT) [4]. Noise of a known amplitude was applied to bunches of protons at 6.5 TeV. From the time the noise was introduced, the bunch was expected to go unstable at a later time; this time delay is referred to as the latency of the instability. The experiment aimed at finding the dependence of the latency on key beam and collider parameters. By understanding these

dependencies, the goal is to better understand how and why the distribution changes in a way that reduces stability.

The experiment was performed over two time slots, June 14$^{\text{th}}$ and July 26$^{\text{th}}$, 2018. On the first date, one successful LHC fill (6791) was tested. A second fill was attempted, but was affected by various delays, and we did not get valuable results. On the second date, two successful LHC fills (6980 and 6981) were tested. These are referred to as fills $1, 2, 3$ in chronological order in the following.

In this note, the beam setup and machine configuration will be presented first. The measured results are detailed next. Then the analysis required to study the latency is explained, including a discussion on how fast the stability threshold is reached. This is followed by an analysis of the measured emittance growth rate from the ADT noise, used to help estimate the noise amplitude.

2 MD Procedure

2.1 Beam setup

2.1.1 Fill 1

Each beam consisted of 10 bunches, injected in a pattern such that there would be no inter-beam interactions. Each beam was separated into 2 groups of 5. The details are given in Tab. 1. The bunches will be referred to by their bucket number. When noise was applied to a group, the bunches experienced noise of relative amplitudes $\{0, 4, 3, 2, 1\}$, in the horizontal plane only. That is, the first bunch in the group is not affected by the noise, such that a threshold value for the octupole current could be established experimentally. These ratios correspond to the peak-to-peak voltage at the ADT kicker.

Table 1: Beam filling scheme and planned noise in fill 1.

Bunch #	1	2	3	4	5	6	7	8	9	10
Bucket in B1	0	300	600	900	1200	1500	1800	2100	2400	2700
Bucket in B2	30	450	750	1050	1350	1650	1950	2250	2550	2850
Group	1	1	1	1	1	2	2	2	2	2
Relative noise [1]	0	4	3	2	1	0	4	3	2	1

[1] Relative noise within the group of 5 at each specific noise level.

2.1.2 Fills 2 and 3

In fills 2 and 3, 13 bunches were injected in each beam, in a pattern such that there would be no inter-beam interactions. The increase from 10 bunches in fill 1 was due to improved operational capabilities of the ADT system between the two dates. Each beam was initially separated into 3 groups of 4, with one bunch as a control group. The details are given in Tab. 2. Because some bunches unexpectedly went unstable close to the stability threshold, the group constellations were varied between the fills. When noise was applied to a group, the bunches experienced noise of relative amplitudes $\{1, 1/2, 1/3, 1/4\}$, in both planes simultaneously. Note the change of relative amplitudes, now it is the inverse of the noise that is linearly spaced. The noise was supposed to be approximately equal in both

planes. Emittance growth rate measurements indicate that the noise was strongest in the horizontal plane.

Table 2: Beam filling scheme and planned noise in fills 2 and 3.

Bunch #	1	2	3	4	5	6	7	8	9	10	11	12	13
Bucket in B1	0	210	420	630	840	1050	1260	1470	1680	1890	2100	2310	2520
Bucket in B2	40	310	520	730	940	1150	1340	1550	1760	1970	2180	2390	2600
Group [1]	0	1	1	1	1	2	2	2	2	3	3	3	3
Relative noise [2]	0	1	1/2	1/3	1/4	1	1/2	1/3	1/4	1	1/2	1/3	1/4

[1] Planned group structure. Varied upon need due to instabilities of individual bunches.
[2] Relative noise within the group of 4 at each specific noise level.

2.2   Experimental setup and execution

The bunches were injected with a large longitudinal separation, and brought to flat top in nominal conditions in all three fills. The ADT was setup so that each channel would affect different bunches. The first group of beam 1 in fill 1 was first acted on with a too strong noise, and the first group of beam 2 was acted on with a too weak noise, due to an issue with the bandwidth. In fill 1, the noise only acted horizontally, while in fills 2 and 3, the noise acted on both planes. Key machine parameters in achieving beam stability were changed in the fills: In fill 1, the octupole current; In fill 2, the chromaticity; In fill 3, the transverse damper gain.

3   Measurements

In this section, the measurements from the experiments will be shown. The emittance was measured continuously with the BSRT. In fills where the BSRT has varied significantly from the wire scanner measurements, the values have been shifted. This is expressly stated in the text. The bunches became unstable horizontally, if not stated otherwise.

Four key machine parameters, relevant for the stability of the bunches, are also presented to discuss the correlation between these parameters and the latency time: (i) The noise amplitude is the peak-to-peak amplitude in volts. The measurement of the absolute value had a limited precision, but the ratios within each group were controlled well. How this can be changed to a noise in units of the rms bunch divergence is discussed in App. A; (ii) The octupole current presented is the measured one; (iii) The transverse damper is represented by the corresponding damping time, in units of number of turns, as discussed in App. B; (iv) The chromaticity is the assigned one in fill 1, and the measured one in fills 2 and 3. Key parameters, both of the bunches and the machine, are collected in App. D. The bunches in fill 1 had intensities around 9×10^{10} p/b, while the bunches in fills 2 and 3 had intensities around 1.1×10^{11} p/b.

3.1   Reading the figures

There are two main kinds of measurement figures. Figures 1,3,5 detail how the emittance of the individual bunches evolved from when the noise was turned on, until they became

unstable or not, for each group of bunches separately. The bunches are always coloured and labelled in order of decreasing noise. The BSRT measurements vary quite a lot, in the presented curves each point corresponds to an average of the closest n values in time, where $n = 15$. The emittance growth from the time the noise was turned on to the time the bunches became unstable has been fitted to linear regressions, which has been plotted on top as dashed lines in the same colours. There are vertical solid lines, also in the same colour, marking where the bunches are considered to have gone unstable. The solid black vertical lines show where the noise was turned on, and the dashed black vertical lines show where the noise was turned off. In some cases, the noise was changed during the experiment to speed up the process. If a key machine parameter was changed during the experiment, this curve is included.

Figures 2,4,6 show the evolution of the key machine parameters for each fill separately. The curves are assigned to the axis labels of the same colour. The vertical damping time and chromaticity is shown in a lighter version of the same colour, and the curves are dashed. The solid black vertical lines mark where a bunch of that beam in that fill became unstable, and can be paired with the vertical coloured lines in the figures detailing the emittance evolution. The dashed black vertical lines mark where a bunch not affected by noise in fill 1, became unstable. Note that the damper is given on a logarithmic scale, while all other values are on a linear scale.

3.2 Fill 1

The emittance measurements for the different groups in fill 1 are given in Fig. 1. They might be slightly underestimated according to corresponding wire scanner measurements, in the order of 10%, but have not been modified. The key machine parameters are collected for each beam separately in Fig. 2. The chromaticity was kept at $Q' = 15$ in both planes, as well as a standard gain corresponding to a damping time of around 200 turns. The octupole current was varied.

Group 1 of beam 1 evolved as shown in Fig. 1a, with $I_{oct} = 452 \, \text{A}$. A too large noise was applied, causing a large emittance growth. It was turned off after approximately 1 minute. The bunches got unstable at a later time. Bunch 600 got unstable at 134.5 min on this x-scale, after I_{oct} was reduced to 339 A. This was the bunch with the smallest intensity and longest bunch length when the noise was on. Otherwise, the bunches became unstable in order of decreasing noise. Bunch 0, which was not affected by the noise, did not became unstable.

Group 2 of beam 1 evolved as shown in Fig. 1b, with a noise reduced by a factor 5 compared to the first value. The octupole current was still 452 A. The bunch experiencing the strongest noise (1800) had a rapid emittance growth, without ever experiencing a coherent instability. The high emittance may have made it less susceptible to instabilities. The other bunches became unstable in order of decreasing noise, bunch 2700 at a reduced octupole current of 370 A. Bunch 1500, which was not affected by noise, became unstable after the octupole current was reduced to 198 A.

Group 1 of beam 2 evolved as shown in Fig. 1c, with an initial noise reduced by a factor 10 compared to the noise applied to group 1 of beam 2. No instabilities or significant emittance growth rates were detected. The noise was therefore doubled and all four affected bunches
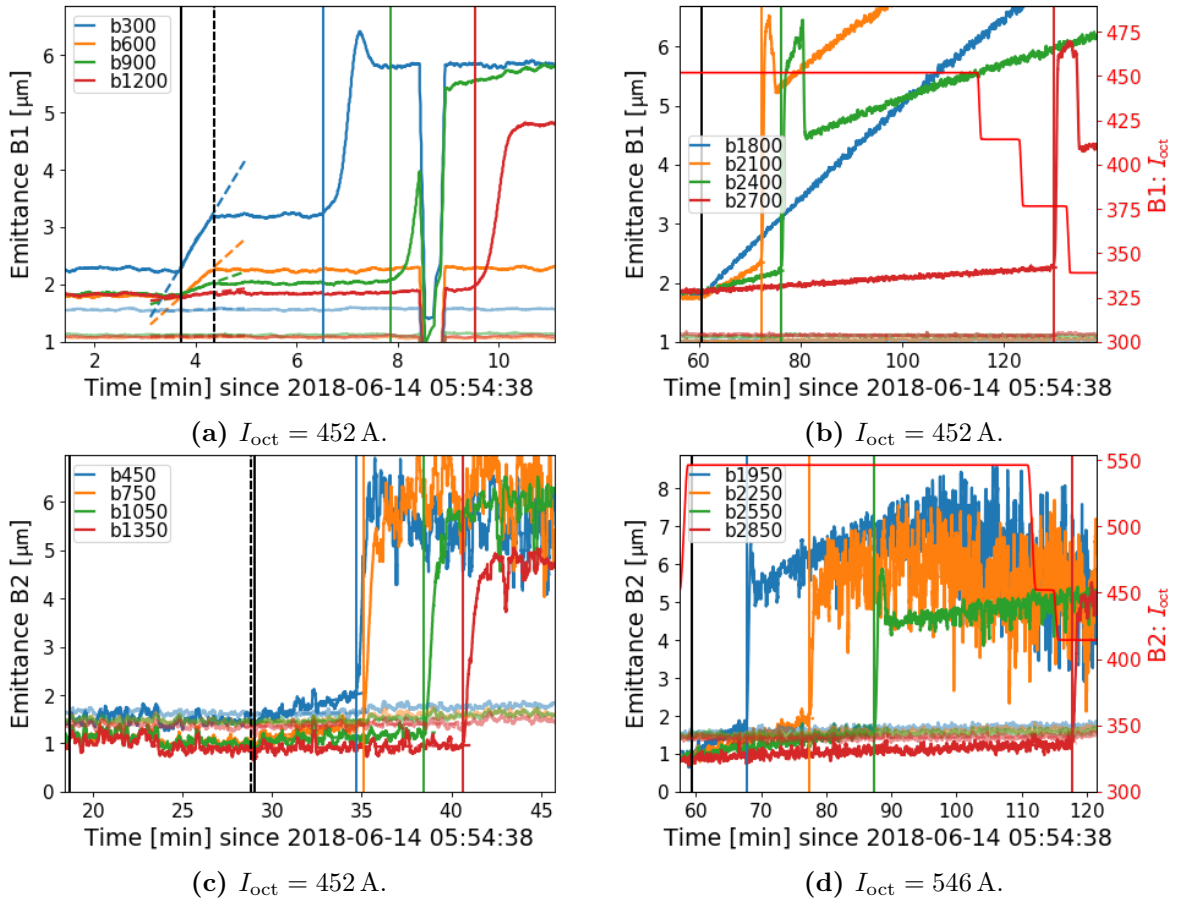
(a) $I_{oct} = 452\,\text{A}$.

(b) $I_{oct} = 452\,\text{A}$.

(c) $I_{oct} = 452\,\text{A}$.

(d) $I_{oct} = 546\,\text{A}$.

Figure 1: Evolution of transverse emittance of bunches in fill 1. The vertical coloured lines show when the bunches are considered unstable. More details are explained in Sec. 3.1.
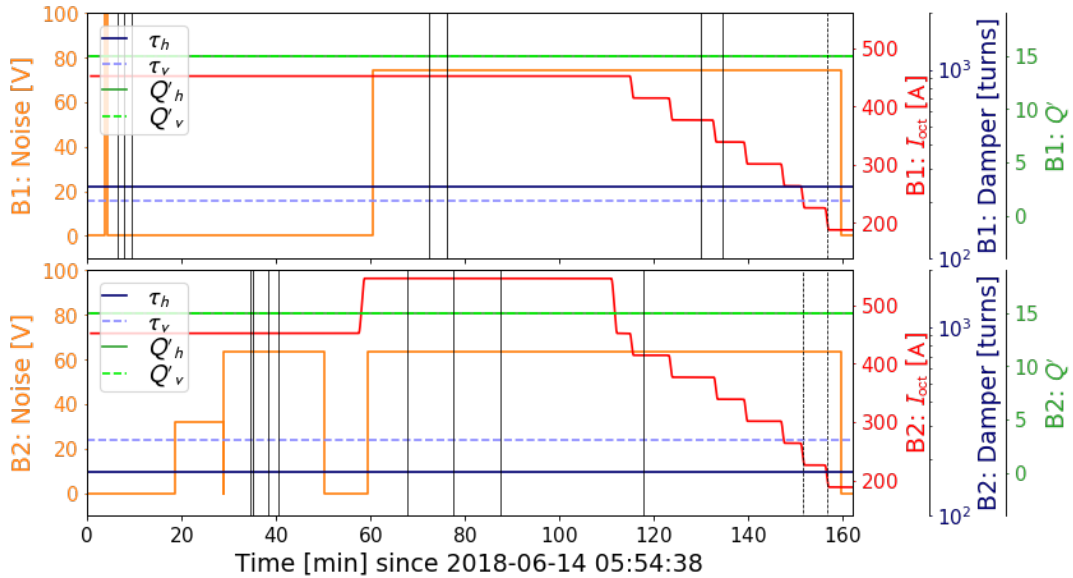

Figure 2: Key machine parameters during fill 1. The vertical black lines show when bunches of that beam became unstable. More details are explained in Sec. 3.1.

6

got unstable in order of decreasing noise within 20 min. The octupole current was 452 A. The latencies are considered from when the stronger noise was applied. Bunch 30, which was not affected by noise, became unstable when $I_{\text{oct}} = 205$ A, during a reduction from 226 A to 188 A.

Group 2 of beam 2 evolved as shown in Fig. 1d. The initial octupole current was increased to 546 A. The bunches became unstable in order of decreasing noise. The bunch with the weakest noise (2850) got unstable at a reduced octupole current of $I_{\text{oct}} = 414$ A. The bunch without noise (1650) got unstable after the octupole current was reduced to $I_{\text{oct}} = 240$ A.

3.3 Fill 2

The emittance measurements for the different groups in fill 2 are given in Fig. 3. The values for beam 2 were significantly underestimated compared to wire scanner measurements. The horizontal emittance has been shifted by 0.6 µm, and the vertical by 0.3 µm. The key machine parameters are collected for each beam separately in Fig. 4. A standard gain, corresponding to a damping time of around 200 turns, was kept fixed throughout the fill. The octupole current was gradually reduced to measure the reduced threshold current. The chromaticity was varied. The first group of both bunches had a chromaticity of about 5, and the second group about 0. The chromaticity was measured at the end of this fill, and it was found that the horizontal chromaticities were 3.35 and 2.79 units too large in beam 1 and 2 respectively, while the vertical chromaticities were -1.80 and -1.77 units too small in the two beams respectively. Two decimals are kept on purpose in these numbers, even if the measurement precision is in the order of single decimals, to avoid adding an additional roundoff error. Hence, the vertical chromaticity was negative for group 2 of both beams, and many bunches became unstable vertically with little or no impact of the noise.

Group 1 of beam 1 evolved as shown in Fig. 3a. The strongest noise was weaker than in fill 1, and the bunches were more stable. The bunches with strongest and third strongest noise became unstable after the octupole current was reduced to 198 A and 151 A respectively. The other two bunches became unstable after the octupole current was reset, and the chromaticity was reduced by 5 units in both planes. The bunches became unstable in order of decreasing noise, except for bunch 420 being later than bunch 630. Bunch 420 had a 7% lower intensity than bunch 630, which could explain this.

All bunches in group 2 of beam 1 became unstable vertically with the negative chromaticity. Group 3 of beam 1 evolved as shown in Fig. 3b. The bunches became unstable vertically in the order of decreasing noise within 10 min, with the exception of the two bunches with the weakest noise. Note that the difference in noise amplitude between these two bunches are 4/3 in this fill, while it was 2 in fill 1. Bunch 2520 had the largest intensity, 10% larger than bunch 2310 and 6% larger than bunch 2100.

Group 1 of beam 2 evolved as shown in Fig. 3c. Similarly to in beam 1, the octupole current had to be reduced significantly before the bunches became unstable. Bunch 310, with the strongest noise, became unstable at $I_{\text{oct}} = 292$ A, while the others were stable until 245 A. The first two became unstable horizontally, while the last two became unstable vertically. The bunches became unstable in order of decreasing noise, with the exception of the two bunches with the weakest noise. Bunch 940 had a 6% higher intensity than bunch 730.
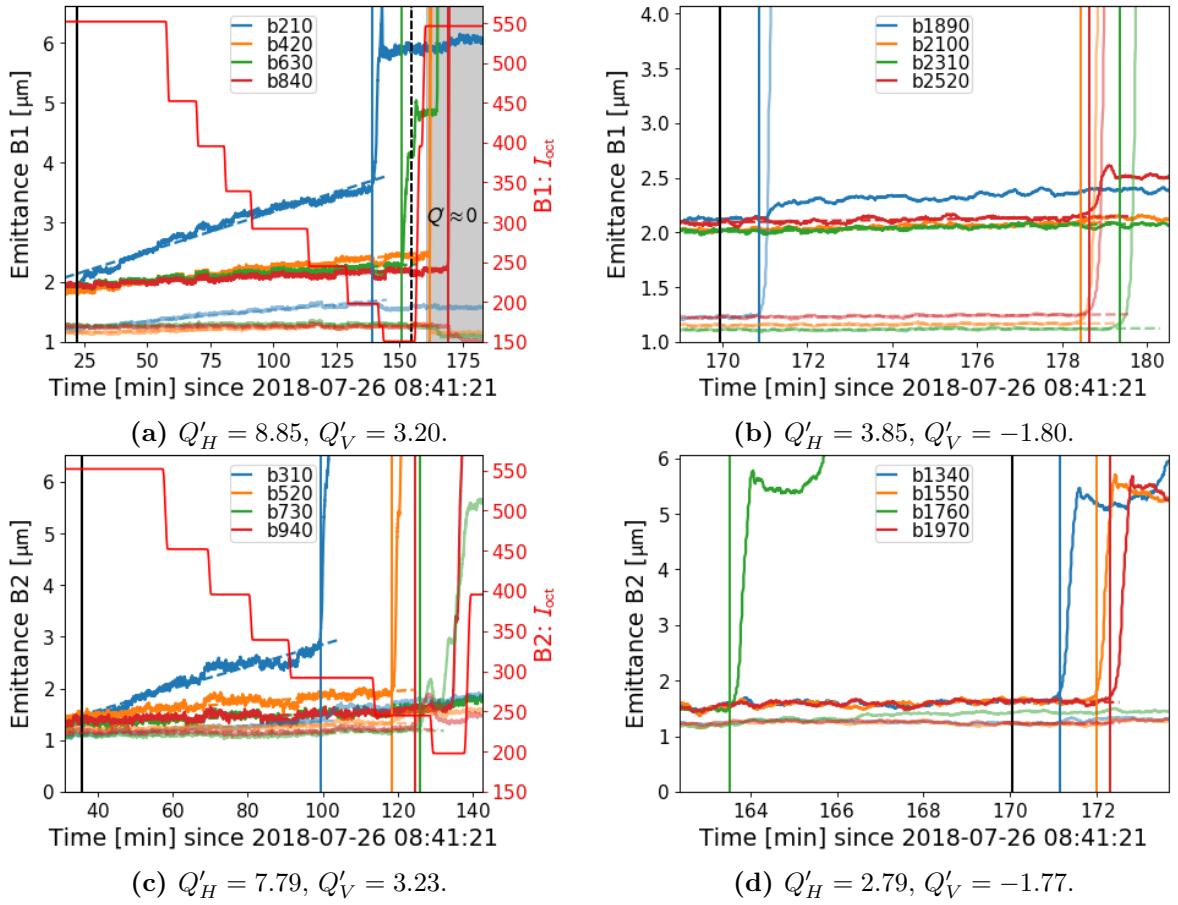
Figure 3: Evolution of transverse emittance of bunches in fill 2. The vertical coloured lines show when the bunches are considered unstable. More details are explained in Sec. 3.1.
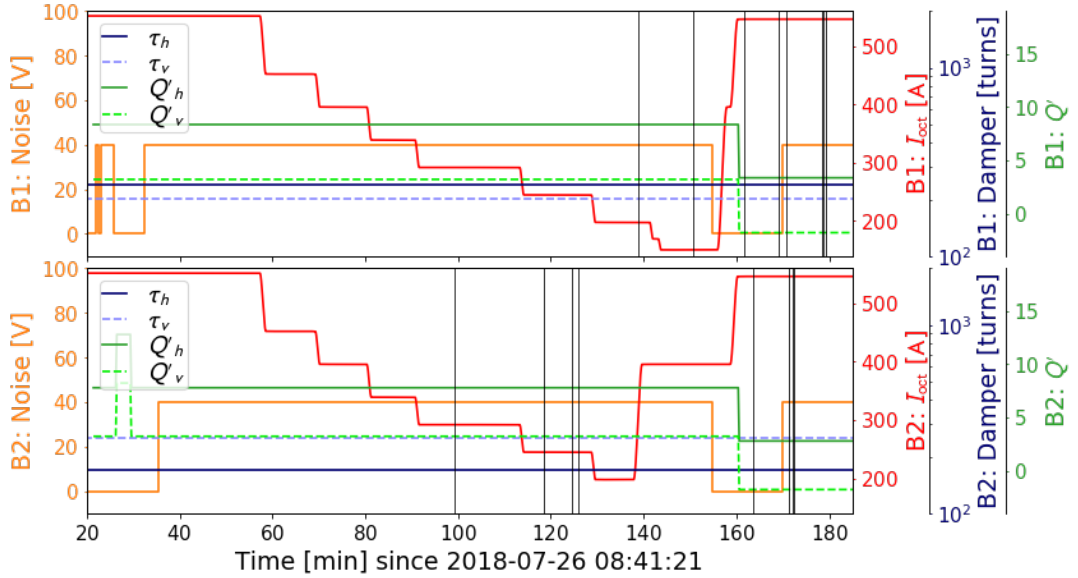

Figure 4: Key machine parameters during fill 2. The vertical black lines show when bunches of that beam became unstable. More details are explained in Sec. 3.1.

8

Group 2 of beam 2 was a hybrid consisting of bunches $\{1340, 1550, 1760, 1970\}$, in order of decreasing noise. The reason for this re-grouping was that all other bunches already had become unstable prior to this. In fact, also bunch 1760 became unstable just before the noise was turned on. This bunch had the smallest emittance of these bunches prior to going unstable, which can explain the reduced stability threshold. The remaining bunches became unstable within two minutes after the noise was turned on, in order of decreasing noise. They seem to have been unexpectedly close to the stability threshold in this configuration.

3.4 Fill 3

The emittance measurements for the different groups in fill 3 are given in Fig. 5. The values for beam 2 were significantly underestimated compared to wire scanner measurements. The horizontal emittance has been shifted by $0.6\,\mu m$, and the vertical by $0.4\,\mu m$. The key machine parameters are collected for each beam separately in Fig. 6. The octupole current was kept larger than $400\,A$. The chromaticity was increased to around 15 units from the values in fill 2. That is, $Q'_H = 18.85$, $Q'_V = 13.20$ for beam 1, and $Q'_H = 17.79$, $Q'_V = 13.23$ for beam 2. In this fill, the gain was changed relative to the standard one that had been used so far. It was first kept as before, giving a third point for the chromaticity dependence studied in fill 2. Then the damper gain was changed, first reduced by a factor 5, then increasing it step by step to twice the standard damper gain.

Group 1 of beam 1 evolved as shown in Fig. 5a. Three bunches became unstable in order of decreasing noise. Bunch 840 had a 5% higher intensity than bunch 630, which might explain the unexpected order of the two. The noise was turned off when bunch 840 became unstable. Hence, the latency of bunch 630 with the noise on, could have been significantly shorter than the measured value.

Group 2 of beam 1 evolved as shown in Fig. 5b, with a 5 times weaker transverse damper than nominal. The weakening of the damper seems to have been positive for the stability, no bunch went unstable with the noise on for more than $30\,min$. The bunches did not go unstable until the damping time was reduced to the nominal one. The bunches became unstable in order of decreasing noise, except for bunch 1050 which had experienced the strongest noise. The noise had led to a significant emittance growth.

Group 3 of beam 1 evolved as shown in Fig. 5c, with a 2 times weaker transverse damper than nominal. None of these bunches either became unstable before the damping time was decreased to the nominal one. These bunches became unstable in the same order as group 2 of beam 1, in the order of reduced noise except for the delay of bunch 1890 which had experienced the strongest noise and a large emittance growth. Note that the emittance growth rate of bunch 1050 was 31% higher than the one of bunch 1890, because the damper gain was lower for group 2.

Group 4 of beam 1 evolved as shown in Fig. 5d, with a 2 times stronger transverse damper than nominal. Group 4 consisted of bunches $\{1470, 1680, 2310, 2520\}$. These were the bunches of groups 2 and 3 that had experienced the weakest noise. They had not yet gone unstable. Bunch 1470 went unstable just before the noise was turned on. The other 3 bunches became unstable within $6\,min$. The threshold in this configuration had most likely already been approached during the first round of noise. The bunches of group 3 became unstable in order of decreasing noise, before the last bunch of group 2 became unstable.
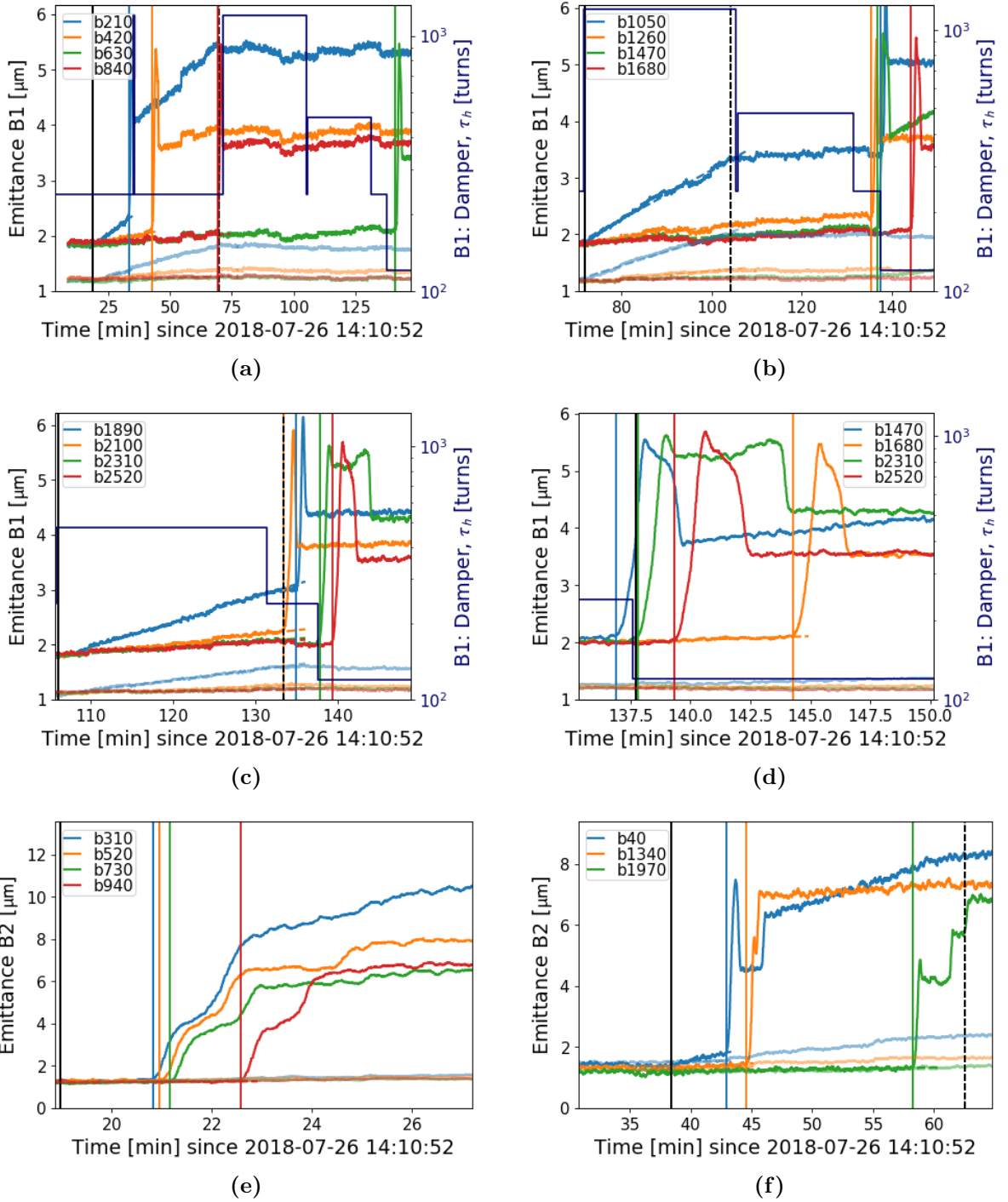
9

Figure 5: Evolution of transverse emittance of bunches in fill 3. The vertical coloured lines show when the bunches are considered unstable. More details are explained in Sec. 3.1.

Group 1 of beam 2 evolved as shown in Fig. 5e, with a nominal gain and $I_{\text{oct}} = 401\,\text{A}$. All bunches became unstable in order of decreasing noise within 4 min. Shortly after these bunches became unstable, several other bunches also became unstable, implying that beam 2 was close to its experimental stability threshold. The octupole current was there-
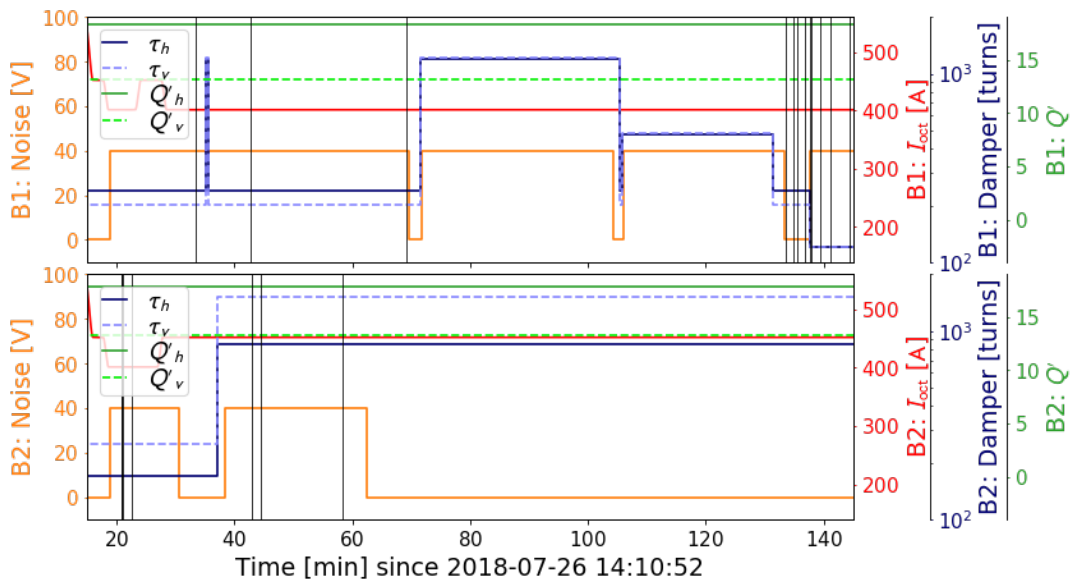
Figure 6: Key machine parameters during fill 3. The vertical black lines show when bunches of that beam became unstable. More details are explained in Sec. 3.1.

fore increased to $452\,\mathrm{A}$. The theoretical threshold was according to `DELPHI` in the interval $I_{\mathrm{oct,thr}}^{\mathrm{the}} \in [200\,\mathrm{A}, 300\,\mathrm{A}]$, as listed in App. D [5].

Group 2 of beam 2 evolved as shown in Fig. 5f, with a 5 times weaker transverse damper than nominal. This group consisted of the last three stable bunches of beam 2, $\{40, 1340, 1970\}$. They became unstable in order of decreasing noise.

3.5 Summary of the measurements

Based on fill 1, it was found that the latency was higher for a higher octupole current, but bunches still became unstable with $I_{\mathrm{oct}} = 546\,\mathrm{A}$. The bunches not affected by the applied noise remained stable until an octupole current close to $200\,\mathrm{A}$, more than a factor 2 lower than in the presence of the noise. Without the noise, this is the experimental stability threshold on the octupole current. It agrees reasonably well with the theoretical stability threshold calculated with `DELPHI`.

Based on the fill 2, and the first group of fill 3, it seems that in the presence of the applied noise, the bunches were more stable with intermediate chromaticity values ~ 5. A chromaticity close to 0 led to vertical instabilities, while a chromaticity around 15 had a shorter latency to a higher threshold octupole current, than for a chromaticity around 5.

Based on fill 3, it seems that the bunches were more stable with a smaller damper gain. This is not expected for a perfect damper. For an imperfect damper, the noise produced by the kick error is proportional to the damper gain, and hence the damper itself can drive this effect. The damper can also have other destabilising effects [6].

11

4 Analysis

In this section, a more detailed analysis of the measurements will be presented. In particular the dependence of the bunch evolution on the key machine parameters that were tested in the three fills. In Sec. 4.1, the raw latency will be presented, which summarises Sec. 3. In Sec. 4.2, the rate of change of the stability threshold due to the applied noise will be analysed. In Sec. 4.3, the emittance growth rate will be analysed, to determine the absolute value of the applied noise.

4.1 Latency of instabilities

The dependence of the measured latency on some key parameters is presented in Fig. 7. The different groups already discussed in Sec. 3 are here collected and presented in a different format. The octupole scan over the two groups in B2 in fill 1 is presented in Fig. 7a. The latency was higher with a higher octupole current. This was expected as the octupole current is required to achieve Landau damping. The simultaneous scan in B1 tested different noise levels instead, and the noise was for the first group turned on before any bunches went unstable. The measured latencies are therefore not comparable and not presented here.

The chromaticity scans over fills 2 and 3 for both beams, are presented in Figs. 7b-c. The latency is shortest for the lowest chromaticity in both beams. Multiple bunches became unstable vertically with the negative vertical chromaticity. The latency was longest with the intermediate chromaticity of ~ 5 units. To make the bunches go unstable with this chromaticity, the octupole current was reduced significantly to $150\,\mathrm{A}$ before ramping it back up and turning off the noise, and still two of the bunches did not go unstable. The apparent reduction of the latency as the chromaticity was further increased to ~ 15 units could also be due to the reduction of the octupole current, denoted in the figures.

The scan of transverse damper gain in both beams in fill 3, are presented in Figs. 7d-e. As noted already in Sec. 3.4, quite some bunches did not go unstable during the allocated time of that group, but rather at a later time during different machine configurations. Hence there are error bars on multiple bunches in B1, starting when the noise was turned off. Remember that the gain was increased for all bunches shortly after the noise was turned off for the affected bunches. It seems that the bunches in this experiment stay stable for longer with a weaker damper gain, opposite of what one naïvely would expect. One purpose of the damper is to damp centroid oscillations, and thereby keeping the bunches stable. However, the predicted stability threshold is inconsequently dependent on the damper gain at these chromaticities [7]. Two effects can explain the lower latency at higher damper gains: (i) the damper is imperfect, and acts as a noise source with amplitude proportional to the gain; (ii) the damper plays a crucial role in explaining how the stability is reduced in presence of an external noise source. The first is known albeit the impact is not quantified, while the second requires further studies.

4.2 Reduction of threshold current

The latency is a measure on how long it takes for the noise in a given configuration to change the beam distribution sufficiently to make the bunch unstable. That is, how long the bunch
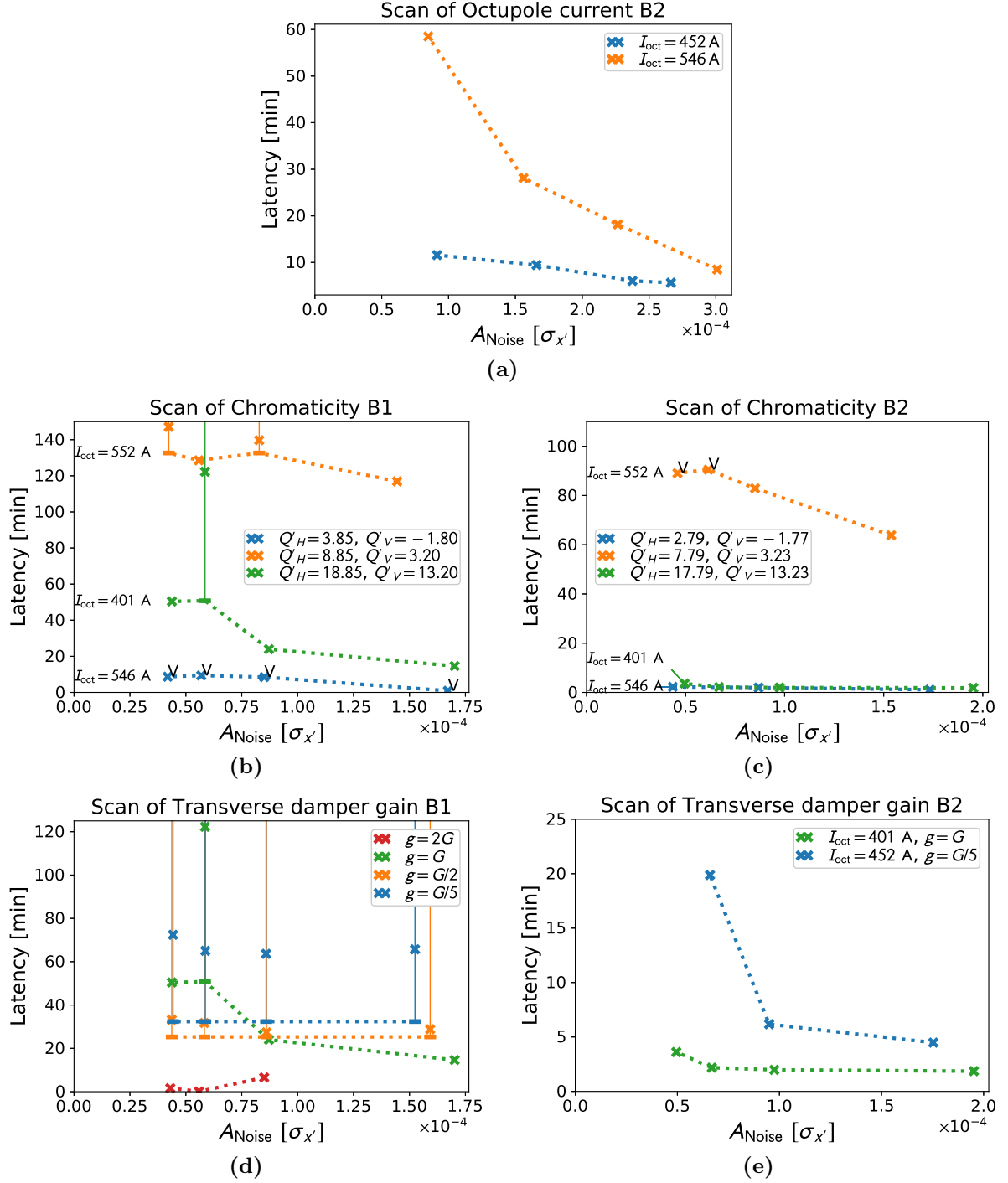
Figure 7: Scan of key machine parameters required to keep the beam stable. The crosses show when the bunches became unstable. If a bunch went unstable vertically, this is annotated by a 'V' next to the cross. The error bar begins where the noise was turned off. The written values of I_{oct} in (b) and (c) are the values when the noise was turned on. The gain is given in units of G, which corresponds to a damping time of ~ 200 turns, and is further explained in App. B.

13

had to be affected by the noise, for the stability threshold octupole current to be increased to the value in the machine. In some cases, when the change was too slow, the octupole current had to be reduced to instead measure how much the octupole current threshold had been increased in a certain amount of time. An important question is therefore what value it had increased from. The empirical threshold was measured for a few bunches during fill 1. However, these values have a precision of $\sim 10\,\mathrm{A}$, and do not take into account the small bunch-to-bunch variations. For instance, when bunches did not go unstable in order of decreasing noise, it was found that they went unstable in order of decreasing intensity or increasing emittance. This is expected from theory [8].

The theoretical threshold, $I_{\mathrm{oct,thr}}^{\mathrm{the}}$, has been calculated for each bunch by use of DELPHI, with key parameters of the bunch and the machine at the time the noise was turned on, t_0, and when the bunch went unstable, t_f [5]. This calculation takes into account the bunch-to-bunch variations that the latency measurements presented in the previous section could not. The empirical threshold, $I_{\mathrm{oct,thr}}^{\mathrm{emp}}$, has been found by measuring I_{oct} when the bunch went unstable. The change of the required octupole current is therefore given as $\Delta I_{\mathrm{oct,thr}} = I_{\mathrm{oct,thr}}^{\mathrm{emp}} - I_{\mathrm{oct,thr}}^{\mathrm{the}}$. This is expected to mostly depend on the machine parameters varied during the experiment

$$\Delta I_{\mathrm{oct,thr}} = \Delta I_{\mathrm{oct,thr}}(Q', I_{\mathrm{oct}}, g, A_{\mathrm{Noise}}, \tau_{\mathrm{noise}}) , \tag{1}$$

where τ_{noise} is the time from the noise was turned on to either the bunch went unstable or the noise was turned off, and A_{Noise} is the standard deviation of the noise in units of sigma of the beam divergence. To first order, we expect $\Delta I_{\mathrm{oct,thr}}$ to be linear with τ_{noise}. Therefore we present in the following $\Delta I_{\mathrm{oct,thr}}/\tau_{\mathrm{noise}}$, and how this depends on the other variables in Eq. (1). This is a rate of change of the stability threshold current.

The dependence of $\Delta I_{\mathrm{oct,thr}}/\tau_{\mathrm{noise}}$ on the key parameters, relative to $I_{\mathrm{oct,thr}}^{\mathrm{the}}(t_f)$ at the time the bunches went unstable, is presented in Fig. 8. The same dependence, relative to $I_{\mathrm{oct,thr}}^{\mathrm{the}}(t_0)$ at the time the noise was turned on, is presented in Fig. 13 in App. C. In some cases, the machine parameters were changed while the noise was on. In these cases, the values when the noise was turned on will be applied. This does not include I_{oct}, which is scanned during the calculation to find the threshold.

A scan of different noise amplitudes is presented in Fig. 8a. This scan was not included in Sec. 4.1. It implies that the rate of threshold change increases faster than linearly with A_{Noise}. Remember that the large noise was only applied for a few minutes, and the bunches went unstable at a later time. Two possible explanations are: (i) The noise initiated a destabilising process that continued after the noise was turned off; (ii) The rate is higher for a bunch that is close to going unstable, and the background noise and wake fields were sufficient to reach the stability threshold.

The octupole scan is presented in Fig. 8b. The points at $A_{\mathrm{Noise}} = 0$ are from the bunches in fill 1 that went unstable without being affected by the external noise source. For these bunches, τ_{noise} is taken to be the time from the beams reached the flat top phase, until the bunches went unstable. There is a clear trend that $\Delta I_{\mathrm{oct,thr}}/\tau_{\mathrm{noise}}$ is lower for a higher I_{oct}. This is good from the point of view of operating the machine, because it is desirable to keep I_{oct} high for the beam to stay stable. There are two possible explanations of this trend: (i) The distribution change causing the change of $I_{\mathrm{oct,thr}}$ is more effective with a smaller tune spread; (ii) The rate is higher for a bunch which is closer to going unstable, possibly due to
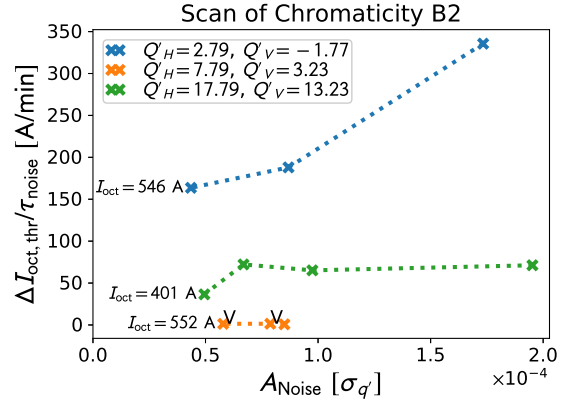
(a) $I_{\text{oct}} = 452\,\text{A}$ for both groups.

(b)
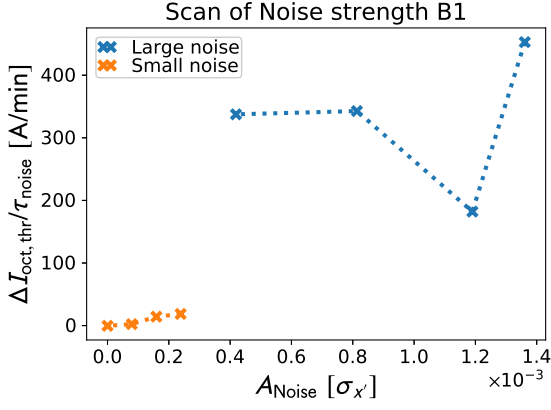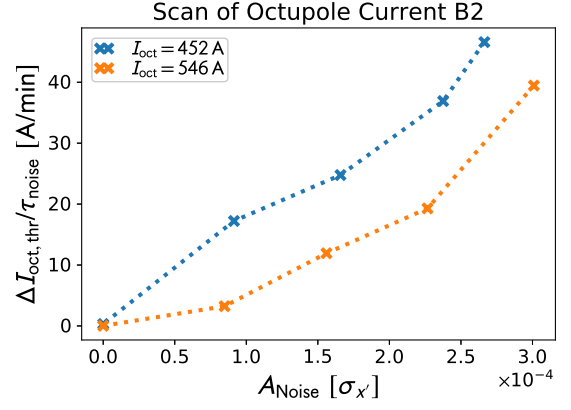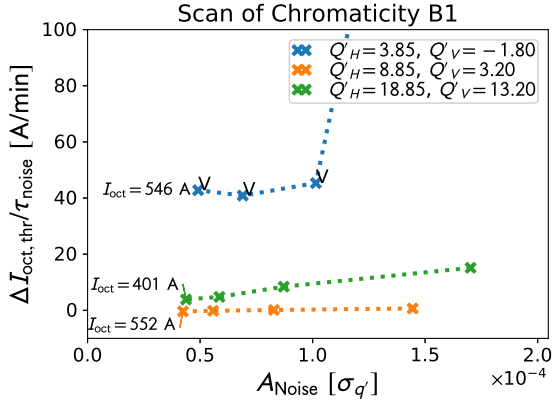
(c) The last point is at $406\,\text{A/min}$.

(d)
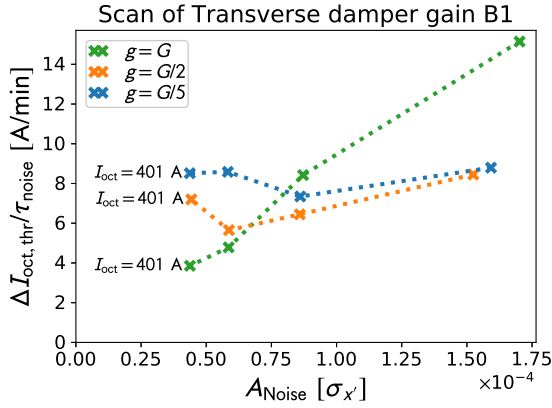
(e)
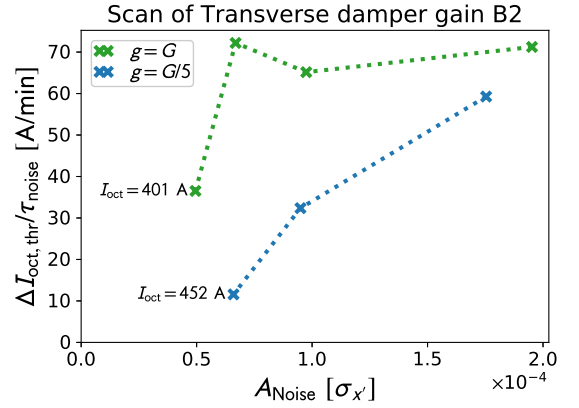
(f)

Figure 8: Increase of threshold I_{oct} per unit of time, $\Delta I_{\text{oct,thr}} = I_{\text{oct,thr}}^{\text{emp}} - I_{\text{oct,thr}}^{\text{the}}(t_f)$. Scans of key machine parameters required to keep the beam stable. The theoretical threshold is for these plots calculated based on the values when the bunches went unstable. If a bunch went unstable vertically, this is annotated by a 'V' next to the cross. The written values of I_{oct} in (c)-(f) are the values when the noise was turned on. The gain labels are further explained in App. B.

an additional impact from the wakefields. There is also a clear trend that the rate increases with A_{Noise}, possibly faster than linearly. This trend is expected qualitatively. However, this trend is not as clear in the rest of the scans presented in Fig. 8.

The chromaticity scan is presented in Figs. 8c-d. The growth rate of the threshold current is close to 0 for $Q' \sim 5$. For the bunches that did not go unstable before the chromaticity was reduced to ~ 0, we have set $I_{\mathrm{oct,thr}}^{\mathrm{emp}} = 151\,\mathrm{A}$. The rate is moderate for $Q' \sim 15$. The rate is higher for $Q' \sim 0$. The similarity in latency between the last two configurations in Fig. 7c, is here shown to correspond to significantly different growth rates of $I_{\mathrm{oct,thr}}$. The bunches are actually predicted to be stable with $I_{\mathrm{oct}} = 0\,\mathrm{A}$ for $Q'_V = -1.80$, but they went unstable almost immediately, both with and without any additional noise. There have previously been strong disagreements between the expected and measured threshold for a chromaticity close to 0 [1]. The chromaticity measurements used have a finite accuracy, and $I_{\mathrm{oct,thr}}^{\mathrm{the}}$ has a strong dependence on Q' close to $Q' = 0$. The largest predicted threshold is with $Q' = 0$, being $I_{\mathrm{oct,thr}}^{\mathrm{the}} \sim 170\,\mathrm{A}$. The predictions with $Q' = 0$ are used for the bunches that went unstable vertically with a negative vertical chromaticity. This leads to lower values for $\Delta I_{\mathrm{oct,thr}}/\tau_{\mathrm{noise}}$. Otherwise, the measured values of the chromaticity have been used for fills 2 and 3.

The damper gain scan is presented in Figs. 8e-f. This scan is less conclusive. The scan in B2 shows that a larger gain corresponds to a higher stability threshold growth rate. However, this difference can be due to the difference in I_{oct}, as it is the same trend as the one shown in Fig. 8b. The scan in B1 shows a different dependence on the gain for small and large noise, and it is non-monotonic in damper gain for large noise. An important trend to note is that no bunch actually went unstable with $g < G$, they only went unstable after the gain was increased back to G or more. The apparent lack of dependence on A_{Noise} for $g < G$ in B1 could be due to this process, that the bunches did not go unstable due to a change of the distribution, but due to a change of the machine configuration after the different noise amplitudes had acted equally long on their respective bunches.

4.3   Emittance growth rate

The relative emittance growth rate is expected to be $0.5 \cdot A_{\mathrm{Noise}}^2 \cdot f_{\mathrm{rev}}$ without a transverse damper. The prefactor will in theory be lower than 0.5 due to the damper [9]. The calculation of A_{Noise} is detailed in App. A. For fill 1, the measured relative emittance growth rates are displayed as a function of A_{Noise}^2 in Fig. 9. The emittance growth rate calculated for $A_{\mathrm{Noise}} = 0$ is the average for all bunches without additional external noise, with error bar equal to standard deviation in these measurements. The error bars for the bunches with nonzero noise are due to the variation in the BSRT measurement of each bunch separately. In this fill, the octupole current was changed moderately between the groups of B2. The relative emittance growth rate is proportional to A_{Noise}^2, but the prefactors are somewhat larger than expected. Based on these measurements, the background noise is negligible compared to the applied controlled noise, since the linear fit crosses close to the origin. There was no noise applied to the vertical plane, and the vertical emittance growth rates were close to 0.

For fill 2, the measured relative emittance growth rates are displayed as a function of A_{Noise}^2 in Fig. 10. There is more variation between the groups in each plane separately in this fill than in fill 1. In this fill, the chromaticity was varied significantly between the groups.

(a) HB1.

(b) HB2.
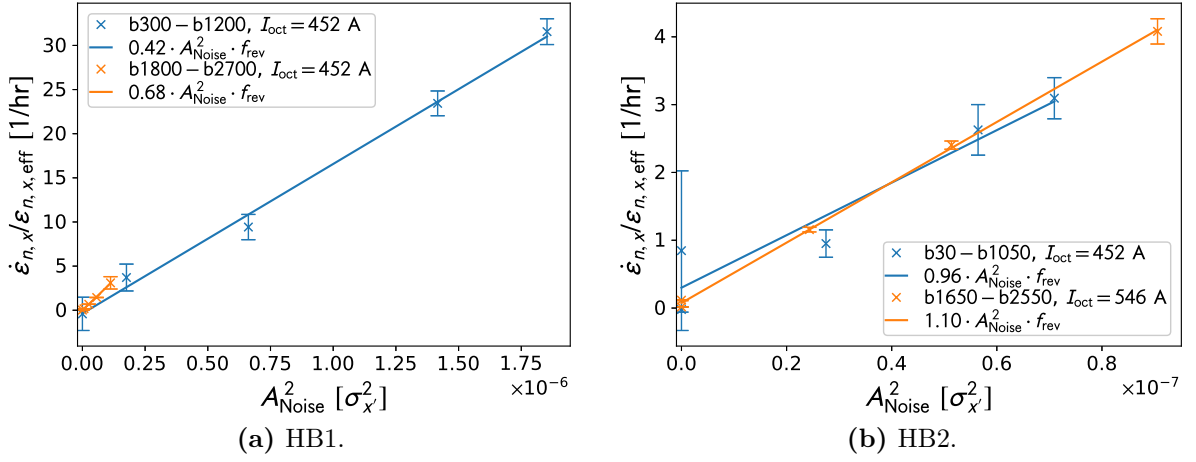
Figure 9: Relative emittance growth rate as a function of the relative noise squared in fill 1. The groups are the same as in Fig. 1, identified by the highest and lowest bucket number.

(a) HB1.

(b) HB2.

(c) VB1.

(d) VB2.

Figure 10: Relative emittance growth rate as a function of the relative noise squared in fill 2. The groups are the same as in Fig. 3, identified by the highest and lowest bucket number.

As seen in App. E, a larger absolute value of Q' corresponds to a larger expected emittance growth rate. For B1, the group with the largest emittance growth rates horizontally, have the smallest emittance growth rates vertically. The measurements of the first group of both

(a) HB1.

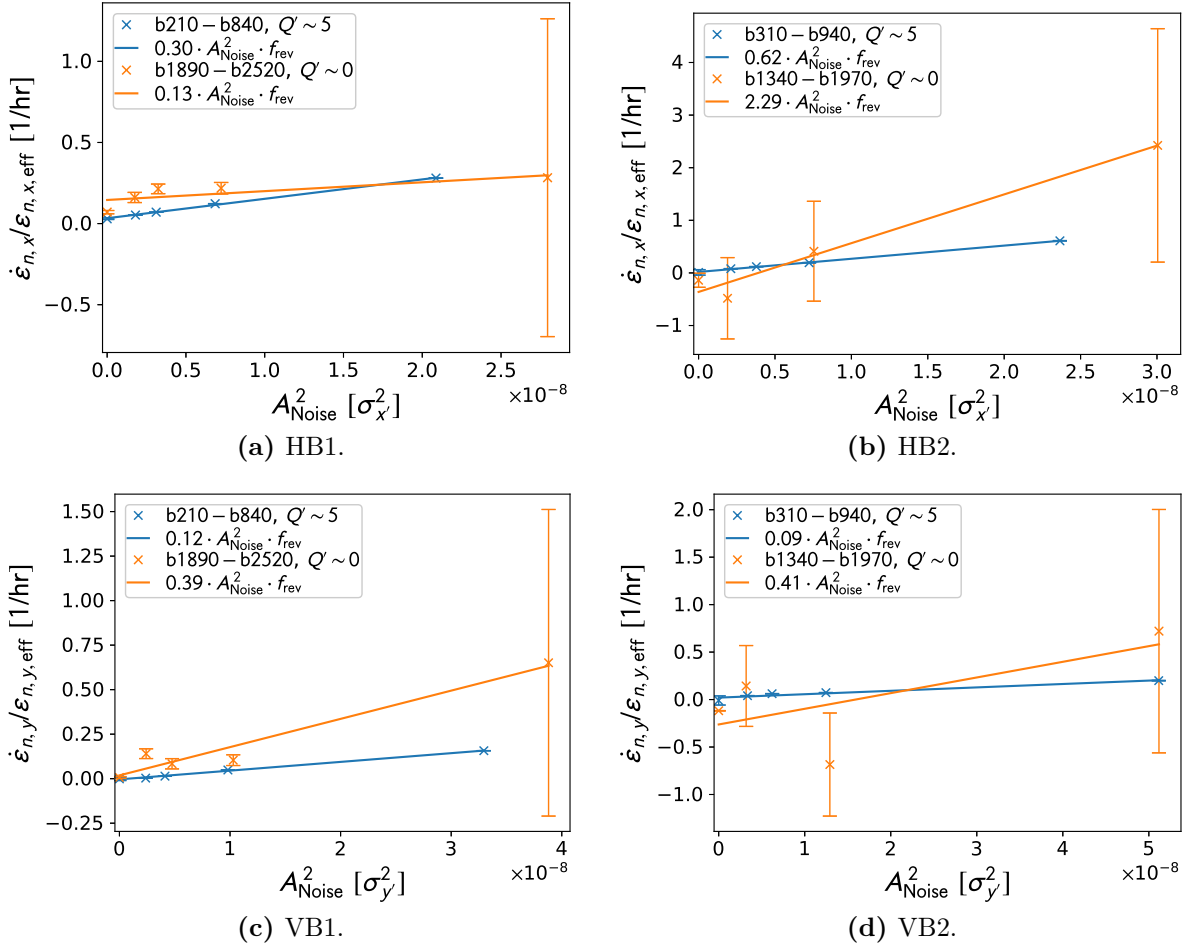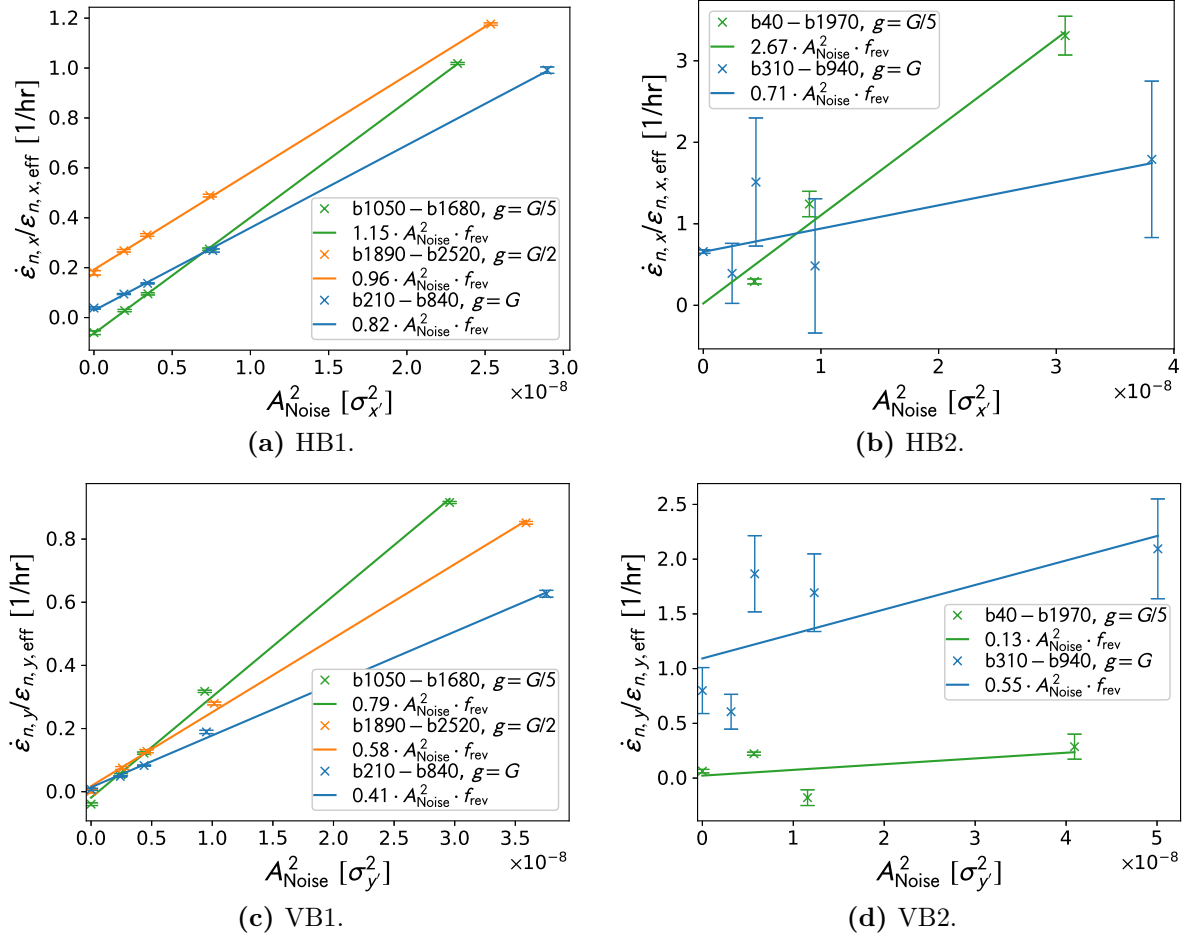**(b)** HB2.

(c) VB1.

(d) VB2.

Figure 11: Relative emittance growth rate as a function of the relative noise squared in fill 3. Disregarding the damper, the emittance is expected to grow like $0.5 \cdot A_{\mathrm{Noise}}^2 \cdot f_{\mathrm{rev}}$. The groups are the same as in Fig. 5, identified with the highest and lowest bucket number.

beams are quite accurate, seen by the error bars, and the linear regression curves go through the origin. The prefactors of the linear fits of these groups are close to or below 0.5, as expected. However, the prefactors were expected to be similar in both planes and beams, which they are not. The larger prefactors in the horizontal plane, can be partially explained by the higher horizontal than vertical chromaticity. The linear fits of the second groups do to a less extent go through the origin, possibly indicating a growth rate independent of the controlled noise. However, due to the inconsistency of this offset and the error bars on the individual points, it is more likely that the offset is due to a limited measurement precision.

For fill 3, the measured relative emittance growth rates are displayed as a function of A_{Noise}^2 in Fig. 11. In this fill, the damper gain was varied significantly between the groups. Except for in the vertical plane of B2, the proportionality factor of the emittance growth rate was reduced as the damper gain was increased. The values for bunches 310-940 in B2 have a significant offset from 0 at zero noise, corresponding to an emittance growth rate without additional noise of $\sim 100\%/h$. This is far away from the average measured transverse emittance growth rate in the LHC in 2018 of about $4\%/h$ [10]. These values were all calculated from measurements of less than $4\,\mathrm{min}$, and are therefore less trustworthy as seen by the significant error bars. This must be due to a drift in the measurement overall.

The individual measurements for B1 have small error bars. There is an offset of the linear fit from zero for $A_{\text{Noise}} = 0$, but this was also measured for the bunches without noises. Especially in Fig. 11a, the correspondence is great. Therefore, the calculated prefactors of the linear fits are good. The offsets at 0 remain to be fully understood.

The main mismatches between the measurements and the theory are the offset from 0 growth rate (or 4%/h) without external noise, and that the proportionality factor is larger than 0.5. There can be multiple sources of these mismatches. The measurement of the emittance with the BSRT could have been adjusted inaccurately, which would lead to an overall over- or underestimation of the emittance. The values in these experiments did vary significantly from the comparative measurements with the wire scanner and was adjusted. The BSRT measurements are also strongly fluctuating for a single bunch. Especially the growth rate measurements over a short time period are inaccurate due to this fluctuation. The measurement of the voltage levels had low precision, with a foreseen error of a factor 2 in either direction. Hence, the square of the noise may be erroneous up to a factor 4. The conversion from voltage to relative noise amplitude may also be inaccurate, both the analytical expression, and the input of the emittance values from the BSRT measurements.

The prefactor is expected to be smaller than 0.5 with a damper. It depends on the ratio between the tune spread and the damper gain. In fill 3, the gain was varied significantly, and the measurements of the emittance growth rates had only a small error bar for B1. A comparison between the predicted and experimental prefactors are given in Fig. 12. The theoretical curve is calculated ignoring the chromaticity, which is non-negligible. The dependence of the prefactor on the chromaticity is not straight forward, as further detailed in App. E. The same configurations as in the machine, using the relevant measured values, have been simulated with COMBI, including chromaticity and a constant synchrotron tune of $Q_s = 0.002$ [11, 12]. The dependence of the experimental points on I_{oct}/g is in the given regime linear, while the simulated values have a small positive curvature. This could indicate that the values $\varepsilon \cdot I_{\text{oct}}/g$ of the experimental values are underestimated. Note that the position on the x-axis also depends on the emittance. Remember from Sec. 3.4 that after

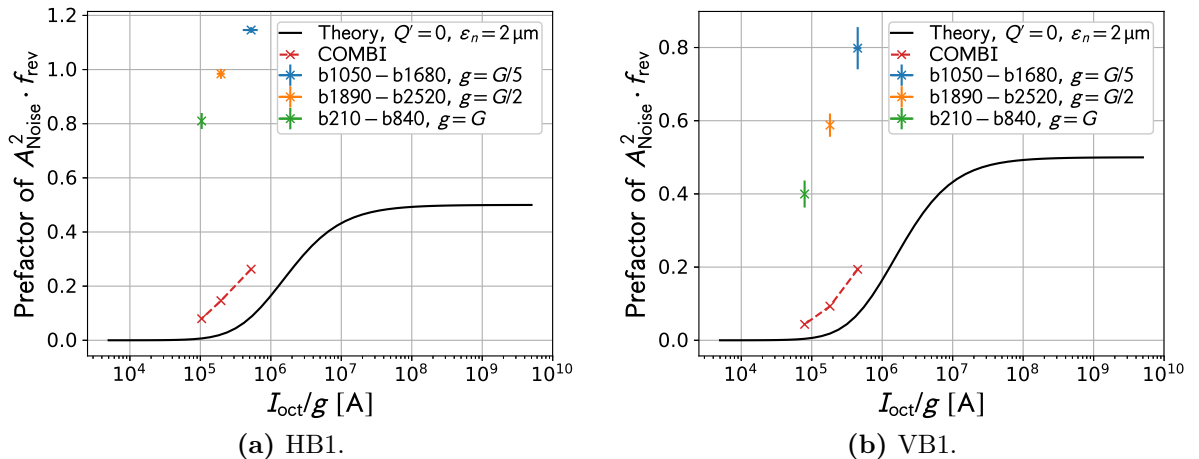**(a)** HB1. **(b)** VB1.

Figure 12: Prefactor study of the emittance growth rates in Fig. 11. Relative emittance growth as a function of the relative noise squared in fill 3. Disregarding the damper, the emittance is expected to grow like $0.5 \cdot A_{\text{Noise}}^2 \cdot f_{\text{rev}}$. The groups are the same as in Fig. 5, identified with the highest and lowest bucket number of the bunch.

comparison with wire scanner measurements, the emittance values from the BSRT for B2 were increased, but the values for B1 were not. The values of I_{oct} and g were both measured with high accuracy. This discrepancy could also be due to uncertain emittance growth rate measurements. The experimental values for the prefactors are in any case larger than 0.5 and about a factor 6 larger than the simulated values. This can be explained by an error in the noise amplitude of a factor 2.4 by itself. If $\varepsilon \cdot I_{\text{oct}}/g$ is in fact underestimated, or the recoherence is imperfect, the error in the noise amplitude would be smaller.

5   Conclusion

In this experiment it has successfully been shown for the first time ever the impact of external noise sources, causing individual bunches to go unstable transversely at octupole currents more than 3 times the expected threshold. The instability mechanism could explain why the observed stability threshold in operation of the LHC is about a factor 2 above the predictions from theory. A similar mechanism may have been the cause of longitudinal instabilities observed in the Tevatron at Fermilab [3]. This MD has improved our qualitative understanding of this subtle mechanism.

The latency of the instabilities, which is the time from the external noise was turned on to the time when the bunches became unstable, has shown some dependencies on key machine parameters. A higher noise amplitude leads to a lower latency, as expected [2]. A higher octupole current leads to a higher latency, as expected. A higher damper gain seems to lead to a lower latency, not as expected. The dependence on chromaticity was non-monotonic, the latency was highest with $Q' \sim 5$, intermediate with $Q' \sim 15$ and lowest with $Q' \sim 0$. The latency also seemed to depend on key bunch parameters, being lower for bunches of higher intensity and lower emittance, as expected [8]. These bunch parameters were not changed deliberately, the trends were seen within the spread due to the limited precision from the injectors.

Another measurement presented in this report is the rate of change of $I_{\text{oct,thr}}$ from the predicted value to the value of I_{oct} in the machine when a bunch went unstable, with the external noise source turned on. This measurement extracts some of the variables in the latency measure, which arose partially due to the limited time with access to the machine. The rate of change was higher with a higher noise amplitude. It was lower with a higher octupole current, implying that the process is faster as the instability threshold is approached. The dependence on chromaticity was again non-monotonic, the rate of change was negligible for $Q' \sim 5$, larger for $Q' \sim 15$, and largest for $Q' \sim 0$. Hence, to reduce the impact of this mechanism, it would be advisable to operate the LHC with $Q' \in [5, 10]$. There is no clear trend in the dependence on the gain. Note that no bunch actually went unstable with a gain less than the nominal one, although they were acted upon with noise with such gains. This was not expected, and will require further analysis to be understood.

The measurement of the noise amplitude had a low accuracy. Hence, the emittance growth rate has also been analysed. The emittance growth rate was found to be proportional to A_{Noise}^2 for the individual groups of bunches, as expected. The prefactors were however larger than expected from theory. Based on this analysis, it has been estimated that A_{Noise} was underestimated by a factor 2.4. During the analysis, it was also found that

20

the dependence of the prefactor on the chromaticity was complicated, due to the decoherence and recoherence caused by the chromaticity.

6 Acknowledgements

References

[1] X. Buffat, G. Arduini, D. Amorim, S. Antipov, L. Barraud, N. Biancacci, L. Carver, F. Giordano, G. Iadarola, K. Li, G. Mazzacano, E. Métral, A. Romano, B. Salvant, M. Schenk, M. Soderen, D. Valuch, L. Mether, T. Pieloni, and C. Tambasco. "Our understanding of transverse instabilities and mitigation tools/strategy". In *8th LHC Operations Evian Workshop*, December 2017. https://indico.cern.ch/event/663598/contributions/2782391/ (Accessed: 23.01.2019).

[2] X. Buffat, D. Amorim, S. Antipov, L. Carver, N. Biancacci, S. V. Furuseth, T. Levens, E. Métral, N. Mounet, T. Pieloni, B. Salvant, M. Soderen, C. Tambasco, and D. Valuch. "The impact of noise on beam stability". In *8th HL-LHC Collaboration Meeting*, October 2018. https://indico.cern.ch/event/742082/contributions/3084844/ (Accessed: 23.01.2019).

[3] V. Lebedev and A. Burov. private communication, Mar. 2019.

[4] D. Valuch. private communication, Mar. 2019.

[5] N. Mounet. "Vlasov Solvers and Macroparticle Simulations". *CERN Yellow Reports: Conference Proceedings*, 1(0):77, 2018. ISSN 2519-8092. URL https://e-publishing.cern.ch/index.php/CYRCP/article/view/757.

[6] E. Métral, D. Amorim, S. Antipov, N. Biancacci, X. Buffat, and K. Li. "Destabilising Effect of the LHC Transverse Damper". (CERN-ACC-2018-129):THPAF048. 4 p, 2018. URL https://cds.cern.ch/record/2648696.

[7] E. Métral, G. Arduini, L. Barranco Navarro, X. Buffat, L. R. Carver, G. Iadarola, K. Li, T. Pieloni, A. Romano, G. Rumolo, B. Salvant, M. Schenk, C. Tambasco, and N. Biancacci. "Measurement and interpretation of transverse beam instabilities in the CERN large hadron collider (LHC) and extrapolations to HL-LHC". (CERN-ACC-2016-0098):TUAM2X01. 7 p, Jul 2016. URL https://cds.cern.ch/record/2199121.

[8] N. Mounet. "The LHC Transverse Coupled-Bunch Instability", Mar. 2012. URL http://cds.cern.ch/record/1451296. CERN-THESIS-2012-055.

[9] V. A. Lebedev. "Emittance growth due to noise and its suppression with the feedback system in large hadron colliders". In *AIP Conference Proceedings 326, 396*, 1995. doi:10.1063/1.47298.

[10] S. Papadopoulou, F. Antoniou, I. Efthymiopoulos, M. Hostettler, G. Iadarola, N. Karastathis, S. Kostoglou, Y. Papaphilippou, and G. Trad. "What do we understand on the emittance growth?". In *Proceedings of the 2019 Evian workshop on LHC beam operation*, 2019.

[11] T. Pieloni, W. Herr, F. Jones, and X. Buffat. Combi (coherent multibunch beam-beam interactions). ABP Computing Web. URL https://twiki.cern.ch/twiki/bin/view/ABPComputing/COMBI. (accessed 30.01.2018).

[12] F. W. Jones, W. Herr, and T. Pieloni. "Parallel beam-beam simulation incorporating multiple bunches and multiple interaction regions", THPAN007. In *Particle Accelerator Conference*, pages 3235–3237. (IEEE, New Mexico, USA, 2007). doi:10.1109/PAC.2007.4440383.

[13] J. Gareyte, J.-P. Koutchouk, and F. Ruggiero. "Landau damping, dynamic aperture and octupole in LHC". (LHC Project Report 91), Feb 1997. URL http://inspirehep.net/record/441038/citations.

[14] S. V. Furuseth and X. Buffat. "Combined effect of damper and decoherence mechanisms". Presentation at ABP-HSC meeting, April 2018. https://indico.cern.ch/event/719980/ (Accessed: 23.01.2019).

Appendix A Transverse Noise

There exists inherent coherent noise sources in the LHC. That is, magnetic fields not produced by the beam itself, which acts equally on all particles in a bunch. One example of such noise is the variation in magnetic field strength due to ripples in the power converter current fed into the dipoles. These sources are not completely mapped, and are not controllable. The LHC transverse damper system (ADT) was used to generate the noise. The noise is generated by pseudo random number generator realized by a Linear-feedback shift register with polynomial of 47th order. It is a white noise with all its properties (it has a normal distribution with constant power spectral density). This is then applied to the beam, where the frequency content is modified by the ADT frequency response. As the bunches in this experiment was well separated, the noise seen by the bunches is still white [4].

The measurement of the peak-to-peak ADT noise voltage level, V_{Noise}, is quite uncertain, the ADT team predicted an error of a factor 2 in either direction. The ratios between the amplitudes of the noise acting on the bunches in a group is however quite accurate. The noise levels are transferred from V_{Noise} to relative amplitudes, A_{Noise} in units of $\sigma_{x'}$, by the following formula

$$A_{\text{Noise}} = \frac{3V_{\text{Noise}}}{2aE\sigma_{x'}} \, , \tag{2}$$

where $a = 52 \times 10^{-3}\,\text{m}$ is the aperture and $E = 6.5\,\text{TeV}$ is the proton energy.

Because A_{Noise}^2 is proportional to the inverse of ϵ_n, we have calculated an effective emittance assuming a linear emittance growth rate as

$$\epsilon_{n,\text{eff}} = \left\langle \frac{1}{\epsilon_n} \right\rangle_t^{-1} = \frac{\epsilon_{n,f} - \epsilon_{n,0}}{\ln(\epsilon_{n,f}/\epsilon_{n,0})} \, , \tag{3}$$

where $\epsilon_{n,0}$ and $\epsilon_{n,f}$ are the normalised emittances when the noise was turned on and off, respectively. This effective emittance is the one used to calculate $\sigma_{x'}$ used in Eq. (2).

Appendix B Transverse Damper

The transverse damper acts by measuring the beam offset, processing the measurement, and at a later time kicking the bunch back towards its closed orbit. If the position is only measured at one location, the kick must be applied at a phase advance of $\pi/2$, such that the position measurement is translated into a measurement on the angle. If the kicker could act instantaneously on the measured angle in the horizontal plane, the impact of the damper on particle j would be

$$x_j' \to x_j' - g_h \cdot \langle x' \rangle \, , \tag{4}$$

where the angle brackets signify that the kick is based on the location of the centroid of the bunch, and g_h is the horizontal damper gain. It can be shown that this leads to a damping of an oscillation, with a damping time

$$\tau_{ip} = \frac{2}{g_{ip}} \, , \tag{5}$$

where $i \in \{1, 2\}$ signifies the beam number, and $p \in \{h, v\}$ signifies the plane.

There is a discrepancy between the gain given to the machine, and the actual gain corresponding to the measured damping time in a linear machine, given by Eq. (5). The damper gains should therefore be multiplied by factors as

$$g_{ip} = g_{ip,LSA} \cdot r_{ip} \; . \tag{6}$$

Based on measurements of the damping time, it was found that the factors are

$$r_{1h} = \frac{1}{6} \quad , \quad r_{1v} = \frac{1}{6} \quad , \quad r_{2h} = \frac{4}{17} \quad , \quad r_{2v} = \frac{2}{15} \; . \tag{7}$$

The gains given in this note are in ratio to a standard gain, G. The horizontal gains $g_x = \{G/5, G/2, G, 2G\}$ correspond to $g_{ip,\text{LSA}} = \{0.01, 0.025, 0.05, 0.10\}$. The vertical gains $g_y = \{G/5, G/2, G, 2G\}$ correspond to $g_{ip,\text{LSA}} = \{0.01, 0.025, 0.06, 0.10\}$. Note that in the vertical plane, the label G refers to $1.2 \cdot G$. Taking into account the factors in Eq. (7), the standard gains G correspond to damping times of ~ 200 turns.

Appendix C   Reduction of Threshold Current

In Sec. 4.2, we presented $\Delta I_{\text{oct,thr}}/\tau_{\text{noise}}$ relative to $I_{\text{oct,thr}}^{\text{the}}$ at the time the bunches went unstable. That is, how much larger I_{oct} was at the time the bunches went unstable than what could be expected from the measured parameters of the bunches at that time, divided by τ_{noise}. It could be argued that it is equally interesting to instead present $\Delta I_{\text{oct,thr}}$ relative to $I_{\text{oct,thr}}^{\text{the}}$ at the time the noise was turned on. This is presented in Fig. 13. The difference in general comes from a small emittance growth and intensity loss with time, leading to a small reduction of the value of $I_{\text{oct,thr}}^{\text{the}}$ with time. Therefore, the values presented here are typically slightly lower.

(a) $I_{\text{oct}} = 452\,\text{A}$ for both groups.

(b)
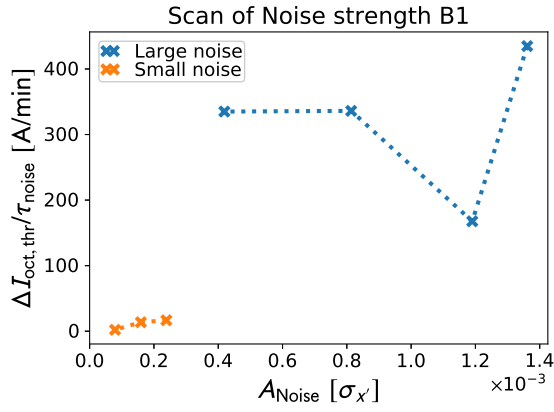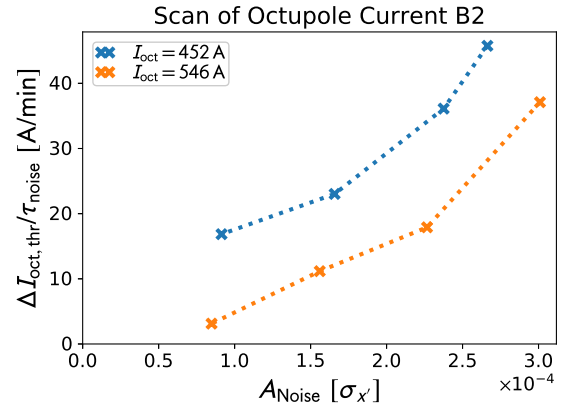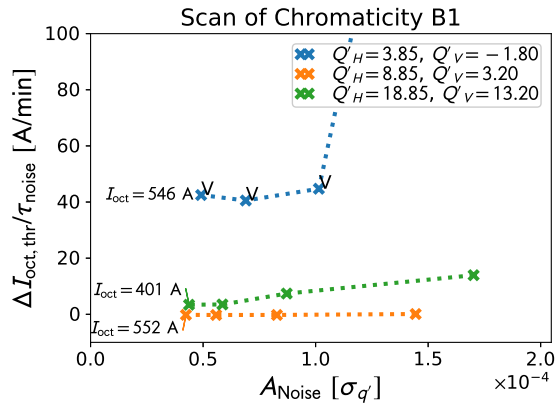
(c) The last point is at $404\,\text{A/min}$.
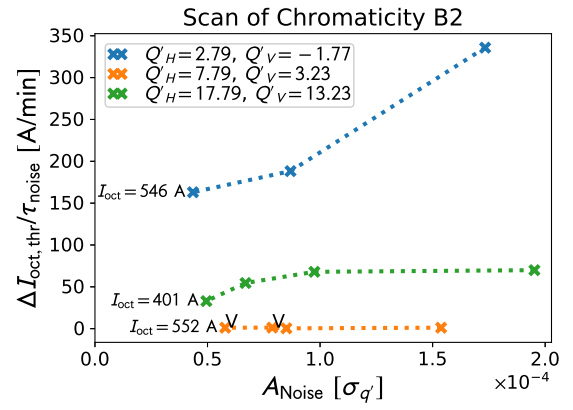
(d)
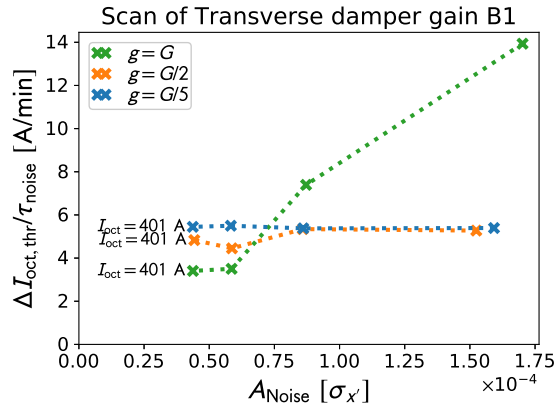
(e)
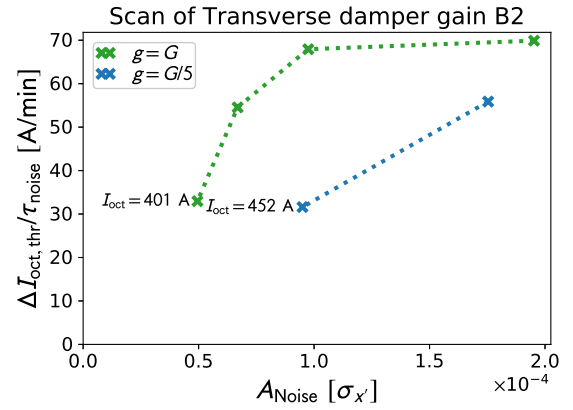
(f)

Figure 13: Increase of threshold I_{oct} per unit of time. Scans of key machine parameters required to keep the beam stable. $I_{\text{oct,thr}}^{\text{the}}$ is for these plots calculated based on the values when the noise was turned on. If a bunch went unstable vertically, this is annotated by a 'V' next to the cross. The written values of I_{oct} in (c)-(f) are the values when the noise was turned on.

Appendix D Numerical Data

Important data of the individual bunches in the experiment is presented here. The listed bunch parameters are the horizontal and vertical normalised emittances, the intensity and the bunch length, at both t_0 when the relevant noise was turned on, and t_f when the bunch went unstable. The predicted stability threshold values of the octupole current ($I_{\mathrm{oct,thr}}^{\mathrm{the}}(t)$), calculated with `DELPHI`, and the experimental octupole current when the bunches actually went unstable ($I_{\mathrm{oct,thr}}^{\mathrm{emp}}$), are also presented [5]. The data from fill 1 are given in Tab. 3, fill 2 in Tab. 4, and fill 3 in Tab. 5. A few predictions have failed, and these values are marked by x's in the tables. Note that, in general, the emittance has grown and the intensity has shrunk a bit, as the time has progressed from t_0 to t_f, leading to, in general, a lower expected threshold current.

Table 3: Important parameters of the relevant bunches in fill 1.

Beam	Bunch	$\varepsilon_{n,x}(t_0)$ [μm]	$\varepsilon_{n,y}(t_0)$ [μm]	$N(t_0)$ [10^{11} p/b]	$4\sigma_s(t_0)$ [ns]	$\varepsilon_{n,x}(t_f)$ [μm]	$\varepsilon_{n,y}(t_f)$ [μm]	$N(t_f)$ [10^{11} p/b]	$4\sigma_s(t_f)$ [ns]	$I_{\mathrm{oct,thr}}^{\mathrm{the}}(t_0)$ [A]	$I_{\mathrm{oct,thr}}^{\mathrm{the}}(t_f)$ [A]	$I_{\mathrm{oct,thr}}^{\mathrm{emp}}$ [A]
1	0	2.61	2.16	0.91	1.12	[1]						
1	300	2.23	1.55	0.91	1.11	2.82	1.55	0.91	1.12	169	158	452
1	600	1.77	1.08	0.89	1.12	2.06	1.08	0.89	1.10	230	221	339
1	900	1.82	1.12	0.94	1.12	1.94	1.12	0.94	1.11	234	229	452
1	1200	1.79	1.10	0.93	1.12	1.82	1.09	0.93	1.14	234	233	452
1	1500					1.91	1.05	0.94	1.09	[2]	245	198
1	1800	1.77	1.02	0.89	1.11	[1]						
1	2100	1.75	1.01	0.94	1.11	2.35	1.00	0.94	1.11	254	230	452
1	2400	1.85	1.09	0.94	1.13	2.22	1.08	0.94	1.09	238	228	452
1	2700	1.84	1.12	0.92	1.11	2.28	1.11	0.91	1.10	227	214	377
2	30					1.91	2.02	0.85	1.04	[2]	155	205
2	450	1.50	1.61	0.88	1.09	1.96	1.60	0.88	1.07	193	188	452
2	750	1.04	1.46	0.93	1.10	1.35	1.42	0.93	1.10	234	229	452
2	1050	0.98	1.45	0.92	1.10	1.18	1.52	0.92	1.10	235	218	452
2	1350	0.81	1.31	0.91	1.10	0.92	1.35	0.91	1.08	257	252	452
2	1650					1.06	1.39	0.88	1.07	[2]	236	240
2	1950	0.89	1.52	0.94	1.10	1.74	1.52	0.94	1.08	232	212	546
2	2250	0.88	1.50	0.88	1.09	1.91	1.48	0.88	1.09	221	196	546
2	2550	0.93	1.50	0.92	1.08	1.62	1.49	0.92	1.09	232	211	546
2	2850	0.82	1.45	0.89	1.09	1.31	1.43	0.88	1.06	232	225	414

[1] Bunches 0 and 1800 of B1 never went unstable, and thus have no values at t_f.
[2] Bunches 1500, 30 and 1650 were not affected by an external noise. Predictions are made only at t_f.

Table 4: Important parameters of the relevant bunches in fill 2.

Beam	Bunch	$\varepsilon_{n,x}(t_0)$ [μm]	$\varepsilon_{n,y}(t_0)$ [μm]	$N(t_0)$ [10^{11} p/b]	$4\sigma_s(t_0)$ [ns]	$\varepsilon_{n,x}(t_f)$ [μm]	$\varepsilon_{n,y}(t_f)$ [μm]	$N(t_f)$ [10^{11} p/b]	$4\sigma_s(t_f)$ [ns]	$I^{\text{the}}_{\text{oct,thr}}(t_0)$ [A]	$I^{\text{the}}_{\text{oct,thr}}(t_f)$ [A]	$I^{\text{emp}}_{\text{oct,thr}}$ [A]
1	210	1.89	1.20	1.06	1.06	3.56	1.63	1.03	1.03	186	122	198
1	420	1.85	1.16	1.02	1.07	2.45	1.28	1.02	1.04	182	135	546 [1]
1	630	1.95	1.28	1.10	1.06	2.29	1.30	1.10	1.05	182	174	151
1	840	1.95	1.27	1.07	1.06	2.18	1.25	1.07	1.04	178	202	546 [1]
1	1890	2.12	1.22	1.15	1.04	2.13	1.23	1.15	1.05	181	180	546
1	2100	2.02	1.15	1.04	1.05	2.08	1.17	1.04	1.05	166	161	546
1	2310	2.01	1.11	1.03	1.05	2.06	1.12	1.03	1.04	165	162	546
1	2520	2.08	1.22	1.12	1.05	2.13	1.25	1.12	1.04	176	174	546
2	310	1.34	1.11	1.04	1.07	2.84	1.38	1.03	1.06	218	x	292
2	520	1.51	1.23	1.12	1.06	1.90	1.32	1.12	1.05	212	182	245
2	730	1.36	1.13	1.04	1.07	1.63	1.25	1.04	1.06	133	112	245
2	940	1.36	1.19	1.12	1.07	1.58	1.29	1.12	1.06	142	123	245
2	1340	1.61	1.24	1.07	1.04	1.64	1.23	1.07	1.05	173	173	546
2	1550	1.63	1.21	1.09	1.07	1.63	1.21	1.09	1.06	178	179	546
2	1760					1.47	1.18	1.08	1.06	[2]	185	546
2	1970	1.62	1.24	1.10	1.05	1.62	1.23	1.10	1.07	179	177	546

[1] Bunches 420 and 840 did not go unstable with $I_{\text{oct}} = 151\,\text{A}$. They went unstable right after the octupole current was increased to 546 A and the chromaticity was decreased by 5 units.
[2] Bunch 1760 went unstable before it was affected by noise, and no prediction has been made for t_0.

Table 5: Important parameters of the relevant bunches in fill 3.

Beam	Bunch	$\varepsilon_{n,x}(t_0)$ [μm]	$\varepsilon_{n,y}(t_0)$ [μm]	$N(t_0)$ [10^{11} p/b]	$4\sigma_s(t_0)$ [ns]	$\varepsilon_{n,x}(t_f)$ [μm]	$\varepsilon_{n,y}(t_f)$ [μm]	$N(t_f)$ [10^{11} p/b]	$4\sigma_s(t_f)$ [ns]	$I^{\text{the}}_{\text{oct,thr}}(t_0)$ [A]	$I^{\text{the}}_{\text{oct,thr}}(t_f)$ [A]	$I^{\text{emp}}_{\text{oct,thr}}$ [A]
1	210	1.82	1.18	1.08	1.12	2.34	1.35	1.08	1.10	197	180	401
1	420	1.86	1.22	1.11	1.09	2.11	1.30	1.11	1.10	224	199	401
1	630	1.84	1.18	1.07	1.08	2.05	1.24	1.07	1.10	223	158	401
1	840	1.89	1.22	1.13	1.08	2.07	1.25	1.12	1.10	229	207	401
1	1050	1.85	1.21	1.10	1.11	3.35	2.00	1.09	1.09	230	128	401
1	1260	1.82	1.16	1.06	1.10	2.18	1.38	1.06	1.07	228	192	401
1	1470	1.82	1.17	1.13	1.08	1.97	1.25	1.13	1.09	257	218	401
1	1680	1.84	1.19	1.13	1.10	1.90	1.21	1.13	1.10	245	168	401
1	1890	1.77	1.07	1.12	1.10	2.98	1.59	1.11	1.09	254	161	401
1	2100	1.78	1.10	1.13	1.10	2.23	1.26	1.13	1.10	254	201	401
1	2310	1.81	1.12	1.14	1.10	2.08	1.20	1.14	1.10	251	167	401
1	2520	1.83	1.14	1.16	1.10	2.06	1.19	1.16	1.10	252	169	401
2	40	1.38	1.51	1.05	1.08	1.76	1.55	1.05	1.08	202	186	452
2	310	1.25	1.21	1.13	1.09	1.33	1.28	1.13	1.08	271	269	401
2	520	1.28	1.25	1.16	1.10	1.31	1.30	1.16	1.08	267	272	401
2	730	1.21	1.19	1.14	1.09	1.24	1.24	1.14	1.11	282	244	401
2	940	1.25	1.21	1.12	1.08	1.26	1.25	1.12	1.08	282	269	401
2	1340	1.23	1.38	1.17	1.09	1.45	1.37	1.17	1.09	257	252	452
2	1970	1.14	1.24	1.04	1.09	1.34	1.31	1.04	1.09	x	222	452

Appendix E   Prefactor of Emittance Growth Rate

Consider a beam subjected to a kick of magnitude k, measured in units of $\sigma_{x'}$, the divergence of the bunch. If the bunch decoheres completely, shifting the centroid back to the origin, it is straightforward to show that the subsequent emittance growth is

$$\frac{\Delta \varepsilon}{\varepsilon_0} = \frac{k^2}{2} \ . \tag{8}$$

With a constant white noise source of impact frequency f, and standard deviation A_{Noise}, k^2 is changed to $A_{\text{Noise}}^2 \cdot f$.

In the presence of a transverse damper of gain g, the entire offset will not lead to emittance growth. Instead, there will be a balance between reducing the offset without emittance growth due to the damper, and reducing the offset with emittance growth due to a tune spread ΔQ, called filamentation. The balance is given by the following equation

$$\frac{\Delta \varepsilon}{\varepsilon_0} = \left\langle \frac{\left(1 - \frac{g}{2}\right)^2 \Delta \mu^2}{\left(\frac{g}{2}\right)^2 + \left(1 - \frac{g}{2}\right) \Delta \mu^2} \right\rangle \cdot \frac{k^2}{2} \ , \tag{9}$$

where $\Delta \mu = 2\pi \Delta Q$ is the shift in phase advance per turn from the centroid of the bunch, and the angle brackets refer to an average over the bunch distribution [9]. In the derivation of this equation, it is assumed that $g < 0.5$, $\Delta \mu \ll 1$ and that $\Delta \mu$ is constant for each particle individually. The prefactor due to the balance between filamentation and damping is in the interval $[0, 1]$. This prefactor is straight forward to calculate for a constant tune distribution, but cannot include the decoherence and recoherence due to chromaticity.

The tune spread in this MD comes mainly from the Landau octupoles and chromaticity. Note that the spread in tune or phase advance per turn, denoted $\Delta \mu$, is the spread from the average value for the bunch. The tune shift from octupoles in the horizontal plane (equivalent for the vertical plane) can be calculated as

$$\frac{\Delta \mu_x}{2\pi} = a_x \cdot (J_x - \langle J_x \rangle) + b_x \cdot (J_y - \langle J_y \rangle) \ . \tag{10}$$

where $J_{x,y}$ is the normalised action, and $a_{x,y}$ and $b_{x,y}$ are prefactors determining the tune spread. They are calculated as [13]

$$\begin{aligned}
a_{x,y} &= 520 \cdot I_{\text{oct}} \cdot \epsilon_{x,y} \ , \\
b_{x,y} &= -380 \cdot I_{\text{oct}} \cdot \epsilon_{y,x} \ .
\end{aligned} \tag{11}$$

Note that it is the geometrical emittance that enters in the expressions in Eq. (11). Ignoring the synchrotron motion, the tune spread from the chromaticity can be calculated as

$$\Delta \mu = 2\pi Q' \cdot \delta \ , \tag{12}$$

where $\delta = \Delta p / p$.

Consider a simple numerical study, using $k = 0.2$, to test the expression in Eq. (9). The relative emittance growth without a damper is equal to $0.5 \cdot 0.2^2 = 0.02$. The theoretical reduction of this value can be calculated numerically with: (i) $Q' = 0$; (ii) $Q' \neq 0$, given that
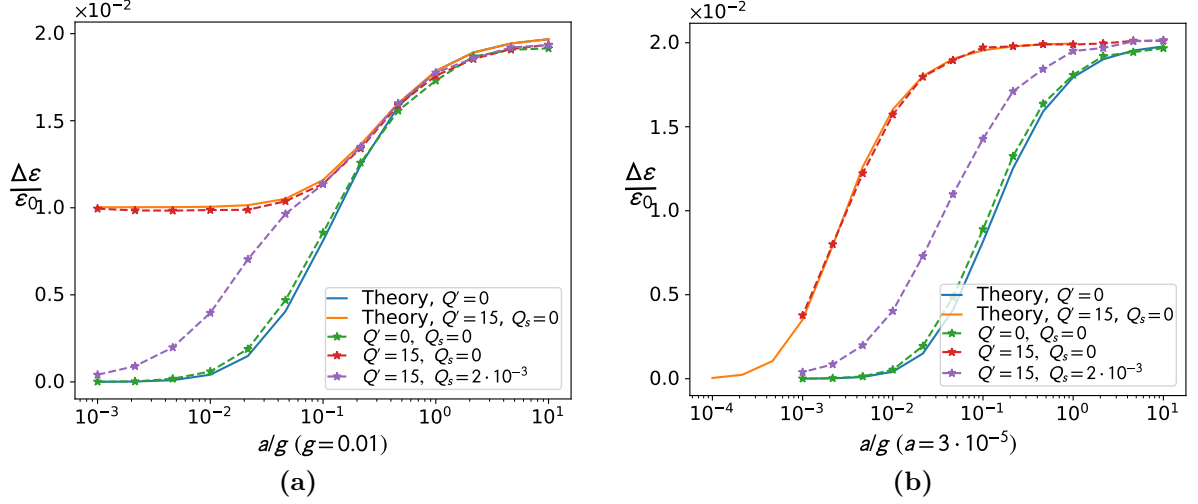
Figure 14: Numerical study of the reduction of emittance growth after full filamentation of a kick due to a tune spread and a damper. In (a) the damper gain is kept fixed while the tune spread from I_{oct} is varied. In (b) it is the damper gain that is varied.

the synchrotron tune $Q_s = 0$. The configurations are simulated with `COMBI` for three cases: (i) $Q' = 0$; (ii) $Q' = 15$ and $Q_s = 0$; (iii) $Q' = 15$ and $Q_s = 0.002$. Case (iii) is the most realistic one. The results are presented in Fig. 14. The theoretical curve for $Q' = 15$ has been calculated with the fitting factor of 0.78 introduced in [14].

With $Q_s = 0$, the chromaticity simply leads to an additional tune spread that increases the filamentation. With $Q_s = 0.002$, one could expect that the recoherence would undo all filamentation due to the chromaticity. This is indeed what happens when $a \to 0$ in Fig. 14a. However, when a is not negligible, the chromaticity leads to an additional emittance growth. This is currently understood as an effect where the chromaticity leads to such a strong tune spread that the centroid amplitude is reduced, and the efficient damper gain is reduced. This effect is negligible when the detuning due to I_{oct} is large, as seen in Fig. 14a. The effect is slightly stronger for a higher damper gain, as seen in Fig. 14b.